



## CHANDRA CHARACTERIZATION OF X-RAY EMISSION IN THE YOUNG F-STAR BINARY SYSTEM HD 113766

C. M. LISSE<sup>1</sup>, D. J. CHRISTIAN<sup>2</sup>, S. J. WOLK<sup>3</sup>, H. M. GÜNTHER<sup>4</sup>, C. H. CHEN<sup>5</sup>, AND C. A. GRADY<sup>6</sup>

<sup>1</sup>Planetary Exploration Branch, Space Exploration Sector, Johns Hopkins University Applied Physics Laboratory,  
11100 Johns Hopkins Road, Laurel, MD 20723, USA; [carey.lisse@jhuapl.edu](mailto:carey.lisse@jhuapl.edu)

<sup>2</sup>Department of Physics and Astronomy, California State University Northridge, 18111 Nordhoff Street,  
Northridge, CA 91330, USA; [damian.christian@csun.edu](mailto:damian.christian@csun.edu)

<sup>3</sup>Chandra X-ray Center, Harvard-Smithsonian Center for Astrophysics, 60 Garden Street,  
Cambridge, MA 02138, USA; [swolk@cfa.harvard.edu](mailto:swolk@cfa.harvard.edu)

<sup>4</sup>Massachusetts Institute of Technology, Kavli Institute for Astrophysics and Space Research,  
77 Massachusetts Avenue, NE83-569, Cambridge, MA 02139, USA; [hgunther@mit.edu](mailto:hgunther@mit.edu)

<sup>5</sup>STScI, 3700 San Martin Drive, Baltimore, MD 21218, USA; [cchen@stsci.edu](mailto:cchen@stsci.edu)

<sup>6</sup>Eureka Scientific and Goddard Space Flight Center, Code 667, NASA-GSFC, Greenbelt, MD 20771, USA; [carol.a.grady@nasa.gov](mailto:carol.a.grady@nasa.gov)

Received 2016 January 14; revised 2016 September 8; accepted 2016 September 23; published 2017 January 10

### ABSTRACT

Using *Chandra*, we have obtained imaging X-ray spectroscopy of the 10–16 Myr old F-star binary HD 113766. We individually resolve the  $1''.4$  separation binary components for the first time in the X-ray and find a total 0.3–2.0 keV luminosity of  $2.2 \times 10^{29} \text{ erg s}^{-1}$ , consistent with previous RASS estimates. We find emission from the easternmost, infrared-bright, dusty member HD 113766A to be only  $\sim 10\%$  that of the western, infrared-faint member HD 113766B. There is no evidence for a 3rd late-type stellar or substellar member of HD 113766 with  $L_x > 6 \times 10^{25} \text{ erg s}^{-1}$  within  $2'$  of the binary pair. The ratio of the two stars' X-ray luminosity is consistent with their assignments as F2V and F6V by Peca et al. The emission is soft for both stars,  $kT_{\text{Apec}} = 0.30\text{--}0.50 \text{ keV}$ , suggesting X-rays produced by stellar rotation and/or convection in young dynamos, but not accretion or outflow shocks, which we rule out. A possible  $2.8 \pm 0.15$  ( $2\sigma$ ) hr modulation in the HD 113766B X-ray emission is seen, but at very low confidence and of unknown provenance. Stellar wind drag models corresponding to  $L_x \sim 2 \times 10^{29} \text{ erg s}^{-1}$  argue for a 1 mm dust particle lifetime around HD 113766B of only  $\sim 90,000$  years, suggesting that dust around HD 113766B is quickly removed, whereas 1 mm sized dust around HD 113766A can survive for  $> 1.5 \times 10^6$  years. At  $10^{28}\text{--}10^{29} \text{ erg s}^{-1}$  X-ray luminosity, astrobiologically important effects, like dust warming and X-ray photolytic organic synthesis, are likely for any circumstellar material in the HD 113766 systems.

**Key words:** astrochemistry – protoplanetary disks – planets and satellites: formation – techniques: spectroscopic – X-rays: stars

### 1. INTRODUCTION

We report here on an analysis of *Chandra* soft X-ray observations of HD 113766, a young (10–16 Myr old, Mamajek et al. 2002; Chen et al. 2006, 2011; Lisse et al. 2008; Peca et al. 2012), F-star binary stellar system of near-solar metallicity ( $\text{Fe}/\text{H} = -0.1$ , Nordstrom et al. 2004), located at a distance of  $123^{+18}_{-14} \text{ pc}$  (8.16 mas *Hipparcos* parallax) from the Earth (Van Leeuwen 2007). Little is known about this system in the X-ray, other than it is a reported unresolved RASS source of luminosity  $2.1 \pm 0.7 \times 10^{29} \text{ erg s}^{-1}$ . On the other hand, in the optical/IR, the system is very interesting. With two component stars of nearly identical age characterized by F spectral types in the Sco-Cen star-forming association, attention had been called to this system, since its association with object IRAS 13037–4545 in the *IRAS* Point Source Catalog was found (Backman & Paresce 1993). More recent work by Meyer et al. (2001), Lisse et al. (2008), and Chen et al. (2005, 2006, 2011) have confirmed that the system exhibits unobscured photospheres and that HD 113766A exhibits one of the largest IR flux excesses measured ( $L_{\text{IR}}/L_* = 0.015$ ), with no detectable  $\text{H}_2$  emission. HD 113766A thus belongs to the class of post-T Tauri objects characterized by young ages of 5–30 Myr, no leftover primordial gas, and large quantities of excess mid-IR emission from circumstellar dust. On the other hand, there is no

evidence for circumstellar dust orbiting the companion, coeval F-star HD 113766B (Meyer et al. 2001), even though studies of young stellar clusters (e.g.,  $\eta$  and  $\chi$  Persei, Currie et al. 2007, 2008) would have led us to expect a few similar dust-forming collisions every Myr in HD 113766B.

Late F-stars are typically strong X-ray emitters at a young age. In fact, the X-ray luminosity function of the Hyades open cluster (age 600 Myr) peaks at late F-stars (Stern et al. 1995). While X-ray emission of O to mid B-type stars is attributed to dissipating shocks in radiation driven winds, and low-mass GKM stars have strong convection leading to an  $\alpha\omega$  or  $\alpha^2$  dynamo, the origin of emission in late B to early F-stars is not so clear. While such stars have a convection zone, the ratio of the X-ray to bolometric flux is much smaller than in typical PMS stars. For example, Collins et al. (2009) find the 10 Myr debris disk host HD 100453 (A9Ve) to have  $\log L_x/L_{\text{bol}} \sim -5.9$ , whereas the typical value for PMS GKM stars is about  $-3.5$  (Feigelson et al. 2005). Intermediate mass stars also appear to have softer spectra than their lower-mass brethren. For example, HD 100453 and the similarly aged 51 Eri (F0V) have coronal temperatures of about 0.2 keV, as opposed to 1–2 keV for similarly aged GKM stars (Feigelson et al. 2006; Collins et al. 2009). Finally, the “FIP-effect” in which elements with first ionization potential below about 10 eV are observed to be enhanced in abundance by a factor of about 3 in the solar corona (Draker et al. 1995), appears to be

absent in some F-stars such as  $\tau$  Boo A (an F7V; Maggio et al. 2011), and Procyon (an F5IV; Raassen et al. 2002 —but see Wood & Laming 2013 for a counter example).

The twin F-stars in the HD 113766 system are thus an interesting and useful couple to study. Close enough (separated by only  $1''.4$ , or 170 AU) to be in the same interstellar medium (ISM) environment, far enough separated that they minimally influence each other's circumstellar environment inside 100 au, and formed at the same time with about the same total mass, they are a natural testbed for trying to understand the mechanisms of exosystem formation. As Myr-old F-stars can be expected to be fast rotators, and more convective and X-ray active than their main-sequence cousins, we would have naively expected both stars to be rapidly rotating, highly convective, and X-ray bright. We thus obtained *Chandra* observations of HD 113766 in 2010, because: (a) the system contained a well known and well studied *IRAS* and *WISE* debris disk, while also being a known RASS source, and therefore observable by *Chandra*, which is a rare combination; (b) using *Chandra*, we could produce the very first resolved maps for the  $1''.4$  wide binary; and (c) it was important to measure the first resolved X-ray spectrum of the system in order to characterize the stellar wind environment of each of its stars, and understand their effect on the known massive dust and ice belts around HD 113766A.

## 2. OBSERVATIONS

In this section, we present the circumstances and results of our 2010 *Chandra* observations of the HD 113766 system. In the next Section 3, we will discuss their implications.

### 2.1. CXO Photometry and Luminosity

We observed the HD 113766 binary using *Chandra* ACIS-S imaging spectroscopy under *Chandra* X-ray Observatory (CXO) program OBSID 12384 on 2010 December 02 UT. For the observation, no filters or gratings were used, and the stars were centered in the 'sweet spot' of the S3 chip. We reprocessed the *Chandra* data with CIAO version 4.8 (Fruscione et al. 2006), which applied the energy-dependent subpixel event repositioning. The total program observing time was 39 ks, and the total on-target observing time was 37.3 ks, in which 1509 total raw photons were detected using a source extraction radius of  $20''$  and an energy filter in the range 0.3–2.0 keV. The extraction region was centered halfway between the two resolved sources' centers. The background was estimated from a large, source-free region on the same chip to be 0.0120 counts per pixel $^{-1}$  in 37.2 ks ( $= 3.2 \times 10^{-7}$  cps/pixel).

After subtracting the background, we determined a total of 1370 source counts, and a source count rate of 0.0366 cps. Using the RASS PSPC rate of  $0.034 \pm 0.014$  cps (*ROSAT* All-Sky Survey, Voges et al. 1999) and assuming a Raymond-Smith coronal plasma model with  $\log T = 6.2$  and solar abundances (Raymond & Smith 1977), W3PIMMS indicated a total HD 113766A+B effective *Chandra* count rate of 0.032 cps (assuming a  $1/4$  subarray to address pileup). Thus, the observed average *Chandra* count rate was within 10% of the RASS count rate extrapolated to the ACIS-S (assuming coronal emission).

The photometric time series (light curve) of the *Chandra* observations is shown for the two sources in Figure 1. The 10:1 relative level of brightness of the two sources remains stable

over the 10.5 hr of *Chandra* observation to within the statistical photon noise. There are qualitatively, however, potential variations in the HD 113766B light curve, which could be periodic. Analyzing the data for possible sinusoidal variations, we find a number of possible solutions with periods ranging from 2.61–2.92 hr, with a best-fit solution at 2.87 hr, a peak-to-peak amplitude of 20%, and  $\chi^2_\nu = 0.98$  for 36 degrees of freedom (dof). However, we also find a null periodic solution with  $\chi^2_\nu = 1.23$ , and note that the 95% confidence limit of the  $\chi^2_\nu$  distribution for 36 dof is 1.42.

While it is tempting to assign this periodicity to rotationally induced variability, the equatorial velocity implied for a  $1.35 R_{\text{Sun}}$  F6V star is  $423 \text{ km s}^{-1}$ , higher than the predicted breakup speed for a solar abundance F-star (for  $M_* = 1.2\text{--}1.6 M_{\text{Sun}}$ ,  $v_{\text{breakup}} \sim 300 \text{ km s}^{-1}$ ). The implied equatorial velocity is also approximately a factor of 2 higher than the fastest known stellar rotators (Głeboccki & Gnaniński 2003; Chen et al. 2011). On the other hand, Chen et al. (2011) have listed a value of  $v \sin i = 93 \text{ km s}^{-1}$  for HD 113766B, and Smith et al. (2012) and Olafsson et al. (2013) have published models of the HD 113766A disk with inclination  $i < 10^\circ$ ; if HD 113766B has a similar inclination, it could have an equatorial rotation velocity in the order of  $400 \text{ km s}^{-1}$ , consistent with the observations. We thus note the *possible* X-ray periodicity in our HD 113766B data for future reference, but also note that we do not understand its source if it is real. It will take a deeper, longer set of X-ray observations than is presented here to robustly verify this possibility.

### 2.2. CXO Imaging

On the S3 chip, we detected two closely spaced X-ray sources in the raw HD 113766 imagery (Figure 2(a)). Image deconvolution was able to better separate these down to the  $0''.2$  scale, clearly showing two separate sources (Figure 2(b)). The centers of these lie  $\sim 1''.4$  apart, and are entirely consistent with the optical and IR locations and separation of  $\sim 1''.4$  for the two stars (Lisse et al. 2008 and references therein), with the optical and IR-brighter HD 113766A to the east, and the optical and IR-fainter but X-ray brighter HD 113766B to the west. The observed flux is very asymmetrically distributed, with  $\sim 90\%$  arising from the optically fainter HD 113766B western binary member, and  $\sim 10\%$  arising from the optically brighter HD 113766A eastern binary member.

In the  $2' \times 2'$  subarray field around the HD 113766 binary pair, we performed a companion search for potential nearby X-ray sources in the field. There is no evidence in our data for any separate, X-ray bright 3rd member of HD 113766 within the  $2'$  of the binary pair with flux greater than three times the image background level. Given the background level of  $\sim 3.2 \times 10^{-7}$  cps per pixel, and an ACIS-S 90% encircled energy radius of 5 pixels, this implies a  $3\sigma$  upper limit for any X-ray object in the field of  $7.5 \times 10^{-5}$  cps (approximately equivalent to  $L_x \sim 5 \times 10^{26} \text{ erg s}^{-1}$ , assuming  $kT = 0.40 \text{ keV}$ ) for an object at the 130 pc distance of HD 113766A/B. This null result is consistent with the lack of any RASS sources in a  $4.2 \times 4.2$  field centered on HD 113766A/B other than the binary system itself (Voges et al. 1999).

Any optically faint, coeval 10–16 Myr old KM stellar or L/T brown-dwarf class object should have been easily detected in the our ACIS-S imaging (see, for example, the strong *Chandra* detection of the M2.5V HR 4796B binary companion to the A0V HR 4796A disk system by Drake

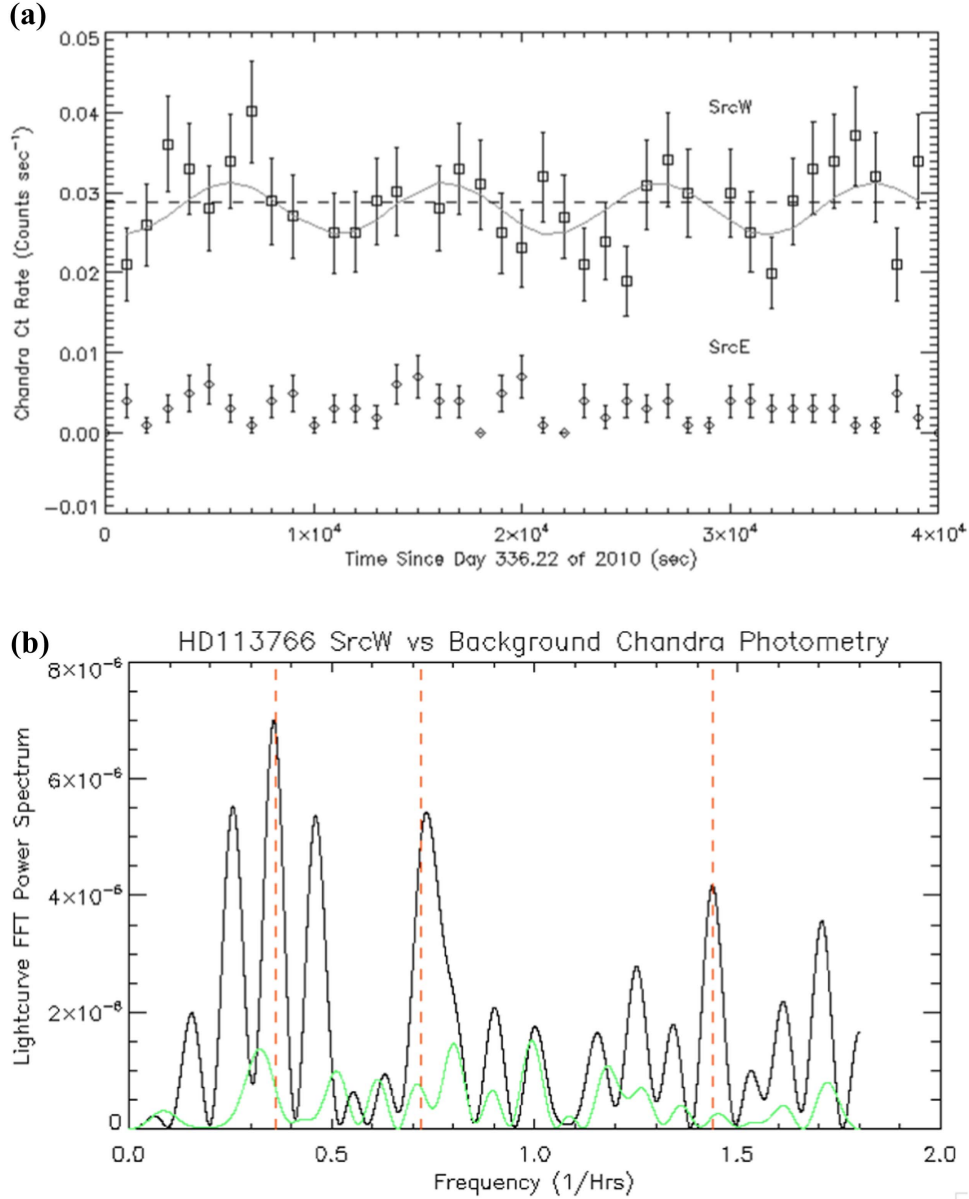


**Figure 1.** (a) *Chandra* ACIS-S photometry of the two X-ray sources detected in the HD 113766 system. All error bars and error estimates are  $2\sigma$ . The background count rate in the *Chandra* point-spread function, as measured far off-source, has been measured with level  $0.01 \pm 0.002$  cps and removed from these curves. The western source, labeled “SrcW,” and identified with HD 113766B, demonstrates a flux of  $0.029 \pm 0.005$  cps (squares), with a possible modulation with sinusoidal periodicity of  $2.8 (\pm 0.15)$  hr and amplitude  $0.0033 (\pm 10\%)$  cps (gray curve) (“possible” since a constant flux model (dashed line) also has  $\chi^2$  value within the 95% confidence limits for our 36 dof light curve). The eastern source, labeled as “SrcE” and identified with HD 113766A (diamonds), is roughly 10 times fainter at  $0.0037 \pm 0.002$  cps. The detection of SrcE is at too low a significance to determine any modulation in the A source. (b) Power spectrum of the HD 113766B *Chandra* light curve (black) compared to that of the background (green), with the location of the possible 2.8 hr periodicity and its  $n = 2$  and  $n = 4$  harmonics marked by the red dashed lines.

et al. 2014). Furthermore, the X-ray spectra we report below for the two stars is much too soft to be produced by an X-ray active KM class stellar object (Collins et al. 2009). While the *Chandra* data cannot rule out very close-in, optically faint substellar companions within  $0''.5$  of the HD 113766 stars, which may be X-ray active, no substantial brown-dwarf-like infrared (IR) excess above the stellar photospheres of either component A or B has been found (Lisse et al. 2008, Olafsson et al. 2013) and  $R - V$  measurements of the stars have put upper limits of  $< 10 M_{\text{Jup}}$  on any close-in companion masses within 50 AU of their primaries (F. Galland et al. 2010, private communication).

### 2.3. CXO Spectroscopy

From the 1370 detected events, we produced a total HD 113766A+B spectrum, extracted over both sources with an  $r = 20$  pixel circular aperture. The combined spectrum is shown in Figure 3(a), and is soft. We estimate a total HD 113766 A+B system luminosity of  $L_x = 2.2 \times 10^{29} \text{ erg s}^{-1}$ . We also extracted separate spectra for the “west” and “east” sources, each over an  $r = 1.6$  pixel circular aperture (Figure 3(a)). After allowing for 30 counts from the brighter western source in the fainter eastern source’s aperture, this provided a reasonable separation of the two

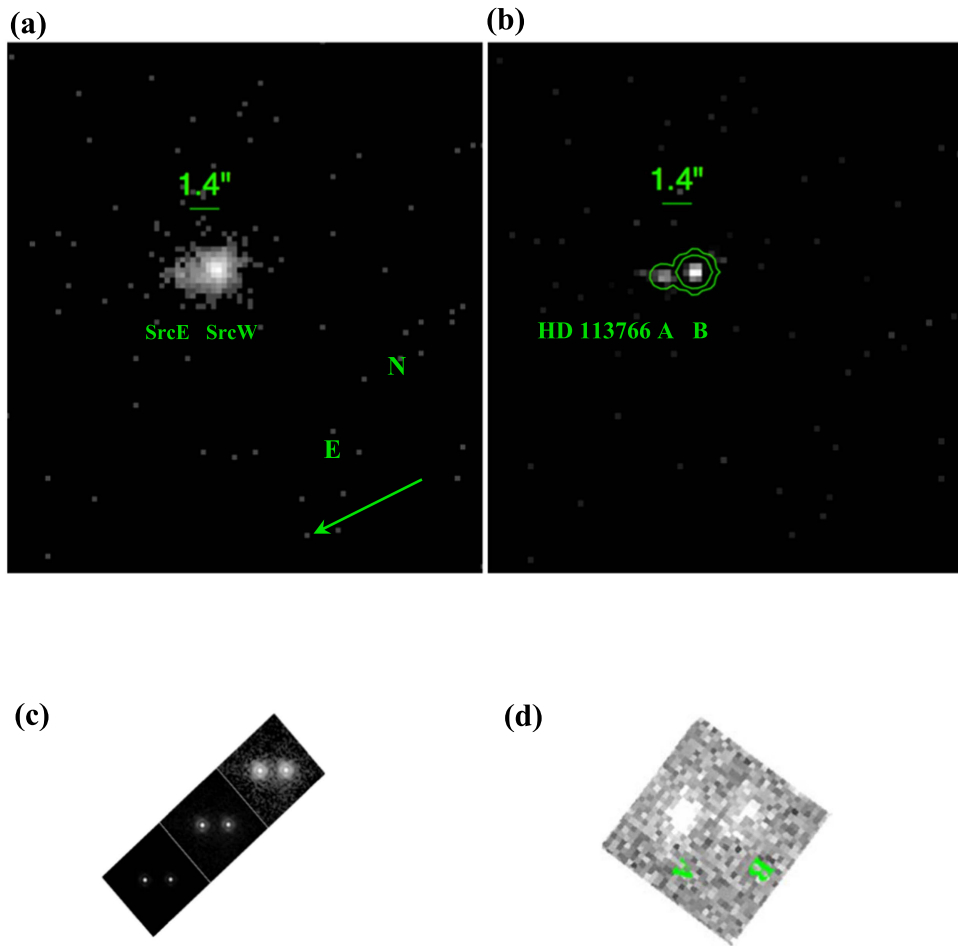


**Figure 2.** *Chandra* ACIS-S imagery of the HD 113766 system. (a, Upper Left) Raw imagery of the system, with all detected photons mapped onto the sky plane. Here, E is to the Left and north is up, implying that the western stellar member of the binary is much more X-ray bright than the eastern member. (b, Upper Right) Deconvolved map of the *Chandra* observations, showing the source separation with  $0''.25$  pixels. (c, Lower Left) *HST*/NICMOS  $1.1\ \mu\text{m}$  image of the system (after Meyer et al. 2001). (d, Lower Right) : *Magellan*  $11\ \mu\text{m}$  image of the system (after Meyer et al. 2001; Smith et al. 2012).

source photon populations, with 1200 counts for the western source and 93 counts for the eastern source in the 0.3–2.0 keV range, implying luminosities  $L_x \sim 2.0 \times 10^{29} \text{ erg s}^{-1}$  for the western source (HD 113766B) and  $L_x \sim 1.6 \times 10^{28} \text{ erg s}^{-1}$  for the eastern source (HD 113766A)

We show model fits to the spectrum of the brighter HD 113766B source (Figure 3(b)). Assuming solar metallicity (following  $\text{Fe}/\text{H} = -0.01$  for HD113766 from Nordstrom et al. 2004), the spectrum can be fitted by an APEC emission model spectrum for collisionally ionized diffuse gas calculated using the ATOMDB code v2.0.1. The best-fit model appears to be very soft, with an APEC temperature of  $0.50 \pm 0.06 \text{ keV}$  (or  $6.7 \pm 0.8 \times 10^6 \text{ K}$ ), and a two-temperature model was not required to fit the data. While four to six times hotter than the effective coronal temperature of the 4.5 Gyr old Sun ( $\sim 0.10 \text{ keV}$ ), it is about the temperature found for other 10–20 Myr solar type stars of similar  $L_x$  (Suchkov et al. 2003; Telleschi et al. 2005). The shape of the spectrum, peaking at  $\sim 0.8 \text{ keV}$ , is also similar to the examples shown in Telleschi et al. (2005) in their X-ray spectral survey of young solar type stars. No strong emission lines above the background are obvious, but this is likely an effect of the coarse energy resolution of  $\sim 50 \text{ eV}$  ( $1\sigma$ ) of the ACIS-S CCD coupled with the low number of total counts. The total detected flux from

0.3–2.0 keV is  $1.4 \times 10^{-13} \text{ erg cm}^{-2} \text{ s}^{-1}$ . The formal derived hydrogen upper limits of  $N_H < 10^{20} \text{ cm}^{-2}$  for the APEC models are consistent with the  $\sim 5 \times 10^{19} \text{ cm}^{-2}$  expected for a stellar source  $\sim 123 \text{ pc}$  distant separated by an intervening interstellar H density of 0.1 particles/ $\text{cm}^3$ , suggesting that there is little in-system H absorption. A small hydrogen column is also consistent with there being little extinction toward the binary, as evidenced by comparing the observed  $B - V$  for the system of  $7.91 - 7.56 = 0.35$  to the predicted intrinsic  $B - V = 0.43$  (Pecaut et al. 2012).

With only 93 total counts, the total number of events obtained for the fainter HD 113766A “east” source is so small that we cannot use binned statistics for spectral fitting. Instead, we use a likelihood-based method (Cash statistic) which is appropriate for Poisson-distributed data. Forcing the  $N_H$  column to be the same as used in our HD 113766B modeling, i.e.,  $N_H < 10^{20} \text{ cm}^{-2}$ , we find that the best fit is a stellar source with a very cool APEC temperature of  $\sim 0.38 \text{ keV}$  or  $5.6 \times 10^6 \text{ K}$ , about 75% the temperature of the B source, and a total flux of  $0.14 \times 10^{-13} \text{ erg cm}^{-2} \text{ s}^{-1}$ , corresponding to an X-ray luminosity  $L_x = 1.6 \times 10^{28} \text{ erg s}^{-1}$  from 0.3–2.0 keV. As the low-count likelihood fitting method does not produce a formal  $\chi^2$  statistic, we cannot derive formal confidence limits, but via forward modeling, Figure 3



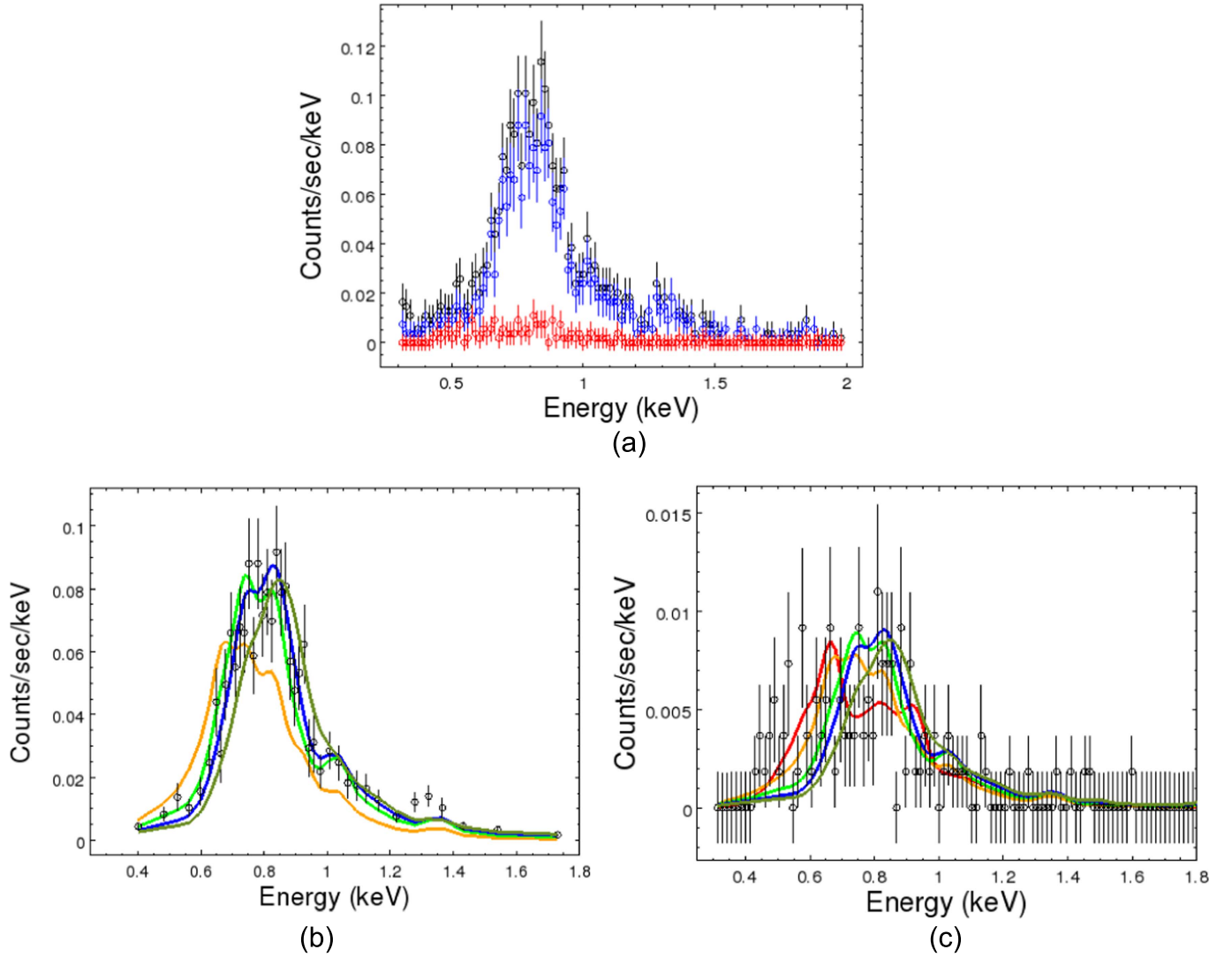


**Figure 3.** *Chandra* ACIS-S spectroscopy of the HD 113766 system. (Above) Spectrum of the combined E+W counts (black circles), bright western source (HD 113766B, blue circles), and fainter eastern source (HD 113766A, red circles). (Below Left) Plot of calibrated ACIS-S X-ray spectrum and APEC coronal model fits to the west source counts (solid colored lines—orange = 0.32 keV, light green = 0.44 keV, dark blue = 0.56 keV, and olive = 0.68 keV). The 0.44 and 0.56 keV models both fit the data equally well. (Below right) Plot of calibrated ACIS-S X-ray spectrum and APEC coronal model fits to the east source counts (solid colored lines—red = 0.20 keV, orange = 0.32 keV, light green = 0.44 keV, dark blue = 0.56 keV, and olive = 0.68 keV). The 0.32 and 0.44 keV models fit the data the best.

shows that temperatures in the range 0.32–0.44 keV (or  $(4.3\text{--}5.9) \times 10^6$  K) produce reasonable fits to the spectra.

### 3. ANALYSIS

In this section, we discuss the first-order implications of our *Chandra* observations of HD 113766 in comparison to X-ray observations of other stars. In the Discussion section, Section 4, we will relate their connections to the bigger picture of debris disk evolution.

#### 3.1. Luminosity Results

Using *Chandra*, we have found an HD 113766 system with *Chandra* count rate and luminosity very close to the published RASS values. The observed X-ray emission can be accounted for by two stellar coronal sources located at the positions of HD 113766A and HD 113766B. HD 113766A is more than  $12\times$  fainter in the X-ray, consistent with the fact that it is the earlier of the two stars (Pecaut et al. 2012 classified

HD 113766A as F1–F3V, and Chen et al. 2011 have classified HD 113766B as F5V–F7V). The fact that HD 113766A is relatively X-ray faint at  $\sim 2 \times 10^{28}$  erg s $^{-1}$ , at the lowest end of the *Hipparcos-ROSAT* survey luminosity range (Suchkov et al. 2003) is also consistent with it being a very early F-star. This is in agreement with the comparison of our *Chandra* HD 113766A results to those found by Feigelson et al. (2006) for 51 Eri, a  $23 \pm 3$  Myr (Bell et al. 2015) F0V star with  $kT = 0.2$  and  $L_x = 1.4 \times 10^{28}$  erg s $^{-1}$ .

Similarly, the  $L_x = 2 \times 10^{29}$  erg s $^{-1}$  *Chandra* luminosity we find for HD 113766B is consistent with the  $L_x \sim 10^{29}$  erg s $^{-1}$  luminosity reported for SAO 206462 by Müller et al. (2011), a young Herbig F8V star with a reported 3.9 hr rotation period. An X-ray luminosity of  $10^{29}$ – $10^{30}$  erg s $^{-1}$  is high for the average main-sequence star, but from the *Kepler* study of the rotation rates of stars (Meibom et al. 2011), as well as previous Hyades and Pleiades measurements (Stauffer et al. 1994; Stern et al. 1995; Güdel 2004), it is plausible for the very young HD 113766 F-stars to be brighter in the X-ray by 1–2

orders of magnitude than their mature main-sequence F-star counterparts.

### 3.2. Imaging Results

Our *Chandra* data has, for the first time, resolved the two stars of HD 113766 in X-rays (Figure 2(a)). Examining in detail our deconvolved *Chandra* X-ray imagery (Figure 2(b)), we do not see any evidence for extended X-ray emission, or emission produced by anything but two point sources to the resolution limit of our mapping ( $\sim 0''.2$ , or 25 AU at 123 pc distance).

The main unusual finding we have for this system is its brightness asymmetry. One of the main questions raised by this was the question of outbursts—i.e., was it possible that HD 113766B was flaring during the *Chandra* observations? Three lines of inquiry suggest that it was not: (a) the achieved count rate for the *Chandra* observations was within 10% of the rate estimated from the 1989 RASS counts, suggesting the system’s X-ray luminosity had been stable over 21 years; (b) the time series of photons detected in our *Chandra* observations show no variability over and above a possible  $\sim 2.8$  hr,  $\sim 20\%$  peak-to-peak amplitude periodicity in the west source; and (c) the temperature of the HD 113766B X-ray spectrum is low compared to the typical 10–100 MK flare temperatures in stellar coronae (Feldman et al. 1995; Kashyap et al. 2002; Shibata & Yokoyama 2002).

Given the incredibly dusty nature of the HD 113766A system and the lack of any dust signature in the HD 113766B system, coupled with the binary pair’s coeval age of 10–16 Myr and the observed asymmetry in X-ray production, a natural inference from our results is that strong X-ray and stellar wind emission destroy and/or accelerate the removal of dust from a stellar system. Support for the latter finding comes from estimates of highly reduced dust lifetimes due to stellar wind drag (Chen et al. 2005, 2006, 2011), and by the anticorrelation between the lifetime of circumstellar dust and primary star X-ray luminosity found in TW Hya by Kastner et al. (2004, 2016). We will discuss this in more detail in Section 4.

### 3.3. Spectral Results

Spectrally, the observed HD 113766B X-ray emission is soft with  $kT \sim 0.50$  keV. This temperature is a factor of a few lower than a typical young G0 (c.f. Preibisch et al. 2005). This is not expected if the source of the flux is an  $\alpha$ - $\Omega$  dynamo, especially for a system in which there is evidence of rapid stellar rotation (Figure 1), unless the shear at the base of the convection zone is especially weak. Other possible effects on the observed spectrum, e.g., that a low coronal electron density or absorption by a large column of nearby H or absorption through the disk of circumstellar material would reduce the luminosity dramatically as well as selectively absorb lower-energy photons, is clearly not consistent with the observed ACIS-S spectrum for HD 113766B. The possibility that the soft spectrum can be attributed to accretion is remote, as (a) Chen et al. (2011) did not report any detectable H-alpha emission in their *Magellan*/MIKE  $R \sim 50,000$  spectra for HD 113766, and (b) because the diskless star of the two in the binary is dominating the X-ray flux. Furthermore,  $R \sim 10,000$  NIR spectroscopy of the HD 113766A+B system using the SPeX instrument at the NASA/IRTF 3 m in 2011 obtained by our group did not detect any CO or HI Brackett  $\gamma$  line emission, which would be

expected in the case of ongoing accretion (Connelly & Greene 2010, 2014; Lisse et al. 2012, 2015). Related NIR measures of outflow activity in our SPeX spectrum, using Fe II, He I, and H<sub>2</sub> lines (Connelly & Greene 2014) are absent, arguing against outflow shocks as a soft X-ray source as well.

## 4. DISCUSSION

F-stars are intriguing objects in the X-ray. At the early end of their type, they are highly radiative and minimal X-ray emitters. At the late end of their type, they are highly convective and are strong X-ray emitters. Myr-old F-stars can be expected to be fast rotators, and more convective and X-ray active than their main-sequence cousins. The HD 113766 system has been alternately described as a 10–16 Myr old F4/F6 or F3/F5 spectroscopic binary by most observers using optical photometry (Holden 1975, 1976; Houk 1978; Olsen & Perry 1984; Hauck & Mermilliod 1998; Mannings & Barlow 1998; De Zeeuw et al. 1999; Fabricius & Makarov 2000; Hoogerwerf et al. 2000; Madsen et al. 2002; Sartori et al. 2003; Hodge et al. 2004; Nordstrom et al. 2004; Chen et al. 2005; Rhee et al. 2008), and so we would have naively expected both stars to be rapidly rotating, highly convective, and X-ray bright. The fact that our east (A) source is  $12\times$  fainter in the X-ray is consistent with it being the earlier of the two stars. The fact that HD 113766A is X-ray faint in the absolute sense at  $\sim 10^{28}$  erg s<sup>-1</sup>, at the lowest end of the *Hipparcos*-*ROSAT* survey (Suchkov et al. 2003), suggests that it is even earlier than F3V to F4V, closer to F2V, and the east component is a late, much more X-ray active F6V star, very much in agreement with Peca et al.’s (2012) recent optical spectroscopic reassessment of the system.

It also suggests that any stellar wind and high-energy stellar radiation effects on circumstellar material and objects are much more important in the HD 113766B system than the HD 113766A system, although the models of Ceisla & Sandford (2012) argue that high-energy irradiation can drive important levels of organic synthesis in any water and organic-rich circumstellar material present in either system—e.g., as has been reported for HD 113766A by Lisse et al. (2008). If local PPDs and the solar system’s history are any guide, this irradiated material is likely to be astrobiologically important, as the larger pieces of it can be reincorporated into asteroids and planetesimals aggregating during the terrestrial planet-building era (which occurred from age 10–100 Myr in our system; Najita et al. 2010; Ercolano & Glassgold 2013; Mendoza et al. 2013; Gudel 2015; Rosotti et al. 2015.). Many of these bodies will later accrete onto the terrestrial planets present in the system during the equivalent of our solar system’s Late Veneer and Late Heavy Bombardment eras (Bottke et al. 2010; Raymond et al. 2013).

### 4.1. Dust- $L_x$ Anticorrelation

We have noted above the highly dusty nature of the X-ray faint HD 113766A system and the dust poor nature of the X-ray bright HD 113766B system. The X-ray observations of TW Hya stars by Kastner et al. (2004, 2016), and the fact that our own Sun is X-ray faint and planet rich versus the *Kepler* G-star average (Basri et al. 2010, 2011), suggests the distinct possibility of a causal connection between circumstellar dust excesses and low X-ray luminosities. Thus, it would seem that the asymmetric X-ray flux found for HD 113766A versus

HD 113766B by *Chandra* for the two coeval, similarly sized F-stars in this system requires a nature or nurture explanation—do dusty disks somehow diminish the observed (but corrected for dust absorption) X-ray flux (nature), or do disks thrive longer in low X-ray and stellar wind flux systems (nurture)?

To address the question of potential X-ray obscuration, it is important to consider the possibility that the circumstellar dust in HD 113766A is strongly attenuating the primary’s coronal emission via absorption and scattering. A simple calculation of  $L_{\text{IR}}/L_{\text{bol}}$  (Lisse et al. 2008 and references therein) shows that while the HD 113766A circumstellar disk is very massive,  $>1$  MMars, it intercepts and scatters at most  $\sim 10^{-3}$  of the bolometric (mostly optical) flux of the star. Assuming normal X-ray scattering cross-sections (Morrison & McCammon 1983) and a thin disk geometry, it is difficult to see how the HD 113766A primary could be emitting roughly the same  $L_x \sim 2 \times 10^{29} \text{ erg s}^{-1}$  as HD 113766B, only to have 90% of this flux absorbed by intervening circumstellar dust. Some enhancement of the observed extinction might be possible if the HD 113766A dust belts (Lisse et al. 2008) were in a fortuitous edge-on viewing situation, à la the Beta Pic system. However, IR imaging of the system does not argue for an unusual edge-on dust disk viewing geometry (Meyer et al. 2001), and the *Spitzer* IRS spectrum of the dust shows strong emission features, arguing against optically thick dust belts. Furthermore, the existence of soft ( $<0.5$  keV) X-rays from HD 113766A (Figure 3) indicates a very small amount of hydrogen gas along the line of sight ( $<10^{20}/\text{cm}^2$ ) and thus a very small  $A_V < 1$ , even for gas to dust ratios as small as 25:1. Thus, dust obscuration of the HD 113766A X-rays is an unlikely reason for the observed X-ray asymmetry, and we again recover the reason for the star’s X-ray luminosity asymmetry as being due to their differing stellar types.

On the other hand, previous authors have noted a possible dusty disk–X-ray luminosity anticorrelation due to the effects of a star’s high-energy irradiation on material in orbit around it. *Chandra* observations of HD 98800, a quadruple system in the 10 Myr old TW Hydrae association, have revealed that the X-ray flux of the dusty binary system HD 98800B is  $4\times$  fainter than its dustless companion HD 98800A (Kastner et al. 2004). Ground-based searches for new 10 and 20  $\mu\text{m}$  excesses around proper-motion and X-ray selected K- and M-type members of the 10 Myr old TW Hydrae association (Weinberger et al. 2004) and around proper-motion, X-ray, and lithium-selected F-, G-, K-, and M-type members of the 30 Myr old Tucana-Horologium association (Mamajek et al. 2004) have been relatively unsuccessful. Recent work by Kastner et al. (2016) targeting the TW Hya M-star population has found an anticorrelation between a star’s photospheric temperature and its  $L_x$  and the amount of IR excess flux arising from circumstellar material surrounding it.

Chen et al. (2005) summarized the possibilities when they wrote in examining their large sample of stars from the young, nearby Sco-Cen stars forming region: “Contrary to expectation, the infrared luminosity appears anti-correlated with X-ray luminosity, except for 30% of the objects that possess neither a *ROSAT* flux nor a MIPS 24  $\mu\text{m}$  excess. The anticorrelation can be naturally explained if stellar wind drag effectively removes dust grains around young stars with high X-ray coronal activity.” Chen et al. (2011) reiterated this possible correlation, stating in the conclusions of their updated  $\sim 400$  star Sco-Cen debris disk survey that they have found a “weak

anticorrelation” between the *ROSAT* flux and the mid-IR flux from a system (the main problems with finding a stronger correlation were stated as the limiting sensitivities of the *ROSAT* survey and the derived stellar mass-loss rates).

#### 4.2. The Effects of Stellar Wind Drag

Chen et al. (2005, 2006, 2011) also noted the unusual nature of the HD 113766 system and its *ROSAT* detection, suggesting the important role that stellar wind drag could have in determining the lifetime of dust in a circumstellar debris disk versus infall onto the primary star. Specifically, they argued that the effects of a dense stellar wind on orbiting dust are similar to those of photons causing Poynting–Robertson drag, with the total contributions of the two mechanisms to the infall velocity  $v_{\text{infall}}$  going as  $v_{P-R} * (1 + c^2 [dM/dt]_{\text{wind}}/L_*)$ . For the Sun, we have  $[dM/dt]_{\text{wind,Sun}} = 2.0 \times 10^{12} \text{ g s}^{-1}$  and  $L_* = 3.9 \times 10^{33} \text{ erg s}^{-1}$ , implying  $v_{\text{infall}} \sim 1.47 v_{P-R}$ .

Photospheric X-ray emission is connected to stellar wind flow, as X-ray emission comes from the breaking of magnetic field lines, and the now open field lines guide energetic plasma away from the star, creating a stellar wind (Osten & Wolk 2015). This connection allows us to estimate the stellar wind mass-loss rate from the stellar X-ray flux using  $[dM/dt]_{\text{wind}} = C * 4\pi R_*^2 F_{x,*}^{1.3}$ , where  $C$  is a constant,  $R_*$  is the stellar radius, and  $F_{x,*}$  is the X-ray flux per unit stellar surface area (Wood et al. 2002, 2005, 2014). The constant  $C$  is determined by scaling from the solar result with  $F_{x,\text{Sun}} = 3.7 \times 10^4 \text{ erg cm}^{-2} \text{ s}^{-1}$  (Mamajek et al. 2002; Wood et al. 2002, 2005).

Assuming  $R_{\text{HD 113766A}} \sim R_{\text{HD 113766B}} = 1.35 R_{\text{Sun}}$  (Lisse et al. 2008 and references therein), with our new *Chandra* results for the binary’s X-ray fluxes we have  $F_{x,\text{HD 113766A}} = 1.4 \times 10^5 \text{ erg cm}^{-2} \text{ s}^{-1}$  and  $F_{x,\text{HD 113766B}} = 1.8 \times 10^6 \text{ erg cm}^{-2} \text{ s}^{-1}$  (compared to the  $F_{x,*} = 9.2 \times 10^5 \text{ erg cm}^{-2} \text{ s}^{-1}$  for both stars of the binary estimated by symmetrically assigning the RASS flux of the system; Chen et al. 2011). This implies  $[dM/dt]_{\text{wind,HD 113766A}} = 2.3 \times 10^{13} \text{ g s}^{-1}$  and  $[dM/dt]_{\text{wind,HD 113766B}} = 5.7 \times 10^{14} \text{ g s}^{-1}$ . With  $L_{\text{HD 113766A}} = 4.4 L_{\text{Sun}}$  for the F2V A-member (Lisse et al. 2008 and references therein; Chen et al. 2011), we find  $v_{\text{infall}} = (2.2 \pm 0.24) v_{P-R}$  for HD 113766A. Assuming  $L_{\text{HD 113766B}} \sim 2.3 L_{\text{Sun}}$  for the F6V B-member (as the model ratio of F6V luminosity to F2V luminosity is  $\sim 0.52$ ), we have  $v_{\text{infall}} = (58 \pm 3.3) v_{P-R}$  for HD 113766B.

We thus find, from our *Chandra* results, that the total drag effects for HD 113766B are  $\sim 26$  times larger as for HD 113766A, and that stellar wind drag effects easily dominate the dynamical repulsive forces for HD 113766B. For HD 113766A, like our solar system, stellar wind drag effects are about equal in effect versus radiative drag forces. However, since  $v_{P-R} \sim L_*$  (Burns et al. 1979), dust in the HD 113766A system still falls onto the primary about 6.6 times faster than in our solar system; but this is still rather slow compared to the 91 times faster than solar system infall rates experienced around HD 113766B.

In absolute terms, we have  $t_{\text{infall}} = t_{\text{infall,solar-system}} * (v_{\text{infall,solar-system}}/v_{\text{infall},*}) \sim 400 * D^2/(0.2/r_{\text{dust}}(\text{um}))\text{years}$   $* (v_{\text{infall,solar-system}}/v_{\text{infall},*})$  (where  $D$  = the distance from the dust particle to the central star and  $r_{\text{dust}}$  is the dust particle radius; Burns et al. 1979). For the warm dust located at  $\sim 1.8$  AU from the HD 113766A primary (Lisse et al. 2008),



assuming it consists of a population of dust of which the largest and longest-lived grains initially present are the abundant  $\sim 1$  mm sized dust grains seen in solar system chondrules and comet trails common to the early solar system, this implies an infall time of  $1.5 \times 10^6$  years for HD 113766A, or a disk clearing time in the order of 1/10th the primary's estimated total age. This suggests that the stability of a dense circumstellar dust disk, massing as least as much as Mars and created by currently ongoing intense asteroidal grinding or planetary accretion (Lisse et al. 2008; Olafsson et al. 2013), is quite plausible. Doing the same calculation for HD 113766B, we find a much shorter infall and disk clearing time of  $\sim 0.9 \times 10^5$  years, less than 1% of the primary's estimated age, and it is not surprising that this system has quickly cleared out any dust created by collisions or impacts onto growing planetary embryos.

In summary, our *Chandra* HD 113766 binary X-ray results, taken together with those for the HD 98800 binary and other singleton debris disks (Kastner et al. 2004, 2016; Chen et al. 2005, 2011; Glauser et al. 2009), suggest that a requirement for circumstellar dust longevity is the lack of a strong primary stellar wind. If this is correct, then we can also expect that on the average young, early F-type stars should have a higher frequency of circumstellar dust disks than young, late-type F-stars as the X-ray luminosity and stellar wind activity increase across the class. It is also interesting to speculate that a relatively low X-ray and solar wind flux may have been the operative case in our early solar system—as suggested by the low activity rate for the Sun versus G-stars found in the *Kepler* sample (Basri et al. 2010, 2011).

## 5. CONCLUSIONS

We have used *Chandra* to obtain imaging spectroscopy of the close ( $1''.4$ , or 170 AU separation), coeval (10–16 Myr old) F-star binary HD 113766 over 38 ks. All three *Chandra* low-energy X-ray measures of this object—imaging, photometry, and spectroscopy—show a system with two detectable sources separated along an E–W line by  $\sim 1''.4$ , with the W source approximately 10 times as bright as the E source. The emission spectrum of each object is well fit by an APEC coronal emission model, although the emission appears to be rather soft for such young stars,  $kT = 0.30$ – $0.50$  keV, leading us to suspect that the coronal magnetic fields are weak in these F-stars. We find asymmetric X-ray emission from the two stellar sources, with the emission from the easternmost, the IR-extended primary object HD 113766A, only  $\sim 10\%$  that of the western star HD 113766B. There is no evidence for a 3rd member of the HD 113766 with mass greater than  $0.1 M_{\text{Sun}}$  within  $2'$  of the AB pair. The X-ray emission from the HD 113766B stronger source may vary with a  $2.8 \pm 0.15$  hr period. For both stars, the strength of the X-ray emission varies inversely with the excess IR flux from circumstellar material. Stellar wind drag models corresponding to the  $L_x \sim 2 \times 10^{29} \text{ erg s}^{-1}$  argue for a dust lifetime around HD 113766B of  $\sim 90,000$  years, suggesting that HD 113766B efficiently clears any secondary dust out of its system, whereas HD 113766A, with  $L_x \sim 2 \times 10^{28} \text{ erg s}^{-1}$  (12 times fainter than B) and dust lifetime  $> 1.5 \times 10^6$  years, could have created the dust seen today anytime within the last Myr. A similar situation has been found for a few other young debris disks, most notably HD 98800 by Kastner et al. (2004). Over the course of 1 Myr, the HD 113766A X-ray emission and stellar

wind irradiation is high enough to drive important levels of organic synthesis in the orbiting circumstellar material, which is rich in water and carbonaceous materials (Lisse et al. 2008; Ceisla & Sandford 2012).

The authors would like to thank J. Kastner, E. Mamajek, and J. Raymond for many useful discussions concerning X-ray emission from young stellar sources. C.M. Lisse gratefully acknowledges support for this work provided by the National Aeronautics and Space Administration through *Chandra* Award Number GO1-12028X issued by the *Chandra X-ray Observatory* Center (CXC). The CXC is operated by the Smithsonian Astrophysical Observatory for and on behalf of the National Aeronautics Space Administration under contract NAS8-03060.

## REFERENCES

- Backman, D., & Paresce, F. 1993, in *Protostars and Planets III* (A93-42937 17-90), ed. E. Levy, J. Lunine, & M. Matthews (Tucson, AZ: Univ. Arizona Press), 1253
- Basri, G., Walkowicz, L. M., Batalha, N., et al. 2011, *AJ*, 141, 20
- Basri, G., Walkowicz, L. M., Batalha, N., et al. 2010, *ApJL*, 713, L155
- Bell, C. P. M., Mamajek, E. E., & Naylor, T. 2015, *MNRAS*, 454, 593
- Botte, W. F., Walker, R. J., Day, J. M. D., Nesvorný, D., & Elkins-Tanton, L. 2010, *Sci*, 330, 1527
- Burns, J. A., Lamy, P. L., & Soter, S. 1979, *Icar*, 40, 1
- Ceisla, F. J., & Sandford, S. A. 2012, *Sci*, 336, 452
- Chen, C. H., Jura, M., Gordon, K. D., & Blaylock, M. 2005, *ApJ*, 623, 493
- Chen, C. H., Sargent, B. A., Bohac, C., et al. 2006, *ApJS*, 166, 351
- Chen, C. H., Mamajek, E. E., Bitner, M. A., et al. 2011, *ApJ*, 738, 122
- Collins, K. A., Grady, C. A., Hamaguchi, K., et al. 2009, *ApJ*, 697, 557
- Connelly, M. S., & Greene, T. P. 2010, *AJ*, 140, 1214
- Connelly, M. S., & Greene, T. P. 2014, *AJ*, 147, 125
- Currie, T., Balog, Z., Kenyon, S. J., et al. 2007, *ApJ*, 659, 599
- Currie, T., Kenyon, S. J., Balog, Z., et al. 2008, *ApJ*, 672, 558
- De Zeeuw, P. T., Hoogerwerf, R., de Bruijne, J. H. J., Brown, A. G. A., & Blaauw, A. 1999, *AJ*, 117, 354
- Drake, J. J., Braithwaite, J., Kashyap, V., Günther, H. M., & Wright, N. J. 2014, *ApJ*, 786, 136
- Draker, J. J., Laming, J. M., Widing, K. G., et al. 1995, *Sci*, 267, 1470
- Ercolano, B., & Glassgold, A. E. 2013, *MNRAS*, 436, 3446
- Fabrizius, C., & Makarov, V. V. 2000, *A&A*, 356, 141
- Feigelson, E. D., Getman, K., Townsley, L., et al. 2005, *ApJS*, 160, 379
- Feigelson, E. D., Lawson, W. A., Stark, M., Townsley, L., & Garmire, G. P. 2006, *AJ*, 131, 1730
- Feldman, U., Laming, J. M., & Doschek, G. A. 1995, *ApJ*, 451, L79
- Fruscione, A., McDowell, J. C., Allen, G. E., et al. 2006, *Proc. SPIE*, 6270, 60
- Glauser, A. M., Güdel, M., Watson, D. M., et al. 2009, *A&A*, 508, 247
- Glebocki, R., & Gnaniński, P. 2003, in *The Catalogue of Rotational Velocities of Stars in Clusters, The Future of Cool-Star Astrophysics: 12th Cambridge Workshop on Cool Stars, Stellar Systems, and the Sun*, ed. A. Brown, G. M. Harper, & T. R. Ayres (Boulder, CO: Univ. Colorado), 823
- Güdel, M. 2004, *A&ARv*, 12, 71
- Güdel, M. 2015, in *EPJ Web of Conferences 102, Protoplanetary Disks: Theory and Modeling Meet Observations*, ed. I. Kamp, P. Woitke, & J. D. Ilee, 00015
- Hauck, B., & Mermilliod, M. 1998, *A&AS*, 129, 431
- Hodge, T. M., Kraemer, K. E., Price, S. D., & Walker, H. J. 2004, *ApJS*, 151, 299
- Holden, F. 1975, *PASP*, 87, 945
- Holden, F. 1976, *PASP*, 88, 52
- Hoogerwerf, R. 2000, *MNRAS*, 313, 43
- Houk, N. 1978, *Michigan Spectral Survey* (Ann Arbor: Dep. Astron., Univ. Michigan), 2
- Kashyap, V. L., Drake, J. J., Güdel, M., & Audard, M. 2002, *ApJ*, 580, 1118
- Kastner, J., Huenemoerder, D. P., Schulz, N. S., et al. 2004, *ApJL*, 605, L49
- Kastner, J., Principe, D. A., Punzi, K., et al. 2016, *AJ*, 152, 3
- Lisse, C., Chen, C., Wyatt, M., & Morlok, A. 2008, *ApJ*, 673, 1106
- Lisse, C., Wyatt, M. C., Chen, C. H., et al. 2012, *ApJ*, 747, 93
- Lisse, C., Sitko, M. L., Marengo, M., et al. 2015, *ApJL*, 815, L27
- Madsen, S., Dravins, D., & Lindgren, L. 2002, *A&A*, 381, 446



- Maggio, A., Sanz-Forcada, J., & Scelsi, L. 2011, *A&A*, **527**, A144
- Mamajek, E. E., Meyer, M. R., Hinz, P. M., et al. 2004, *ApJ*, **612**, 496
- Mamajek, E. E., Meyer, M. R., & Liebert, J. 2002, *AJ*, **124**, 1670
- Mannings, V., & Barlow, M. J. 1998, *ApJ*, **497**, 330
- Meibom, S., Barnes, S. A., Latham, D. W., et al. 2011, *ApJL*, **733**, L9
- Mendoza, E., Almeida, G. C., Andrade, D. P. P., et al. 2013, *MNRAS*, **433**, 3440
- Meyer, M. R., Backman, D., Mamajek, E. E., et al. 2001, *BAAS*, **33**, 1420
- Morrison, R., & McCammon, D. 1983, *ApJ*, **270**, 119
- Müller, A., van den Ancker, M. E., Launhardt, R., et al. 2011, *A&A*, **530**, A85
- Najita, J. R., Carr, J. S., Strom, S. E., et al. 2010, *ApJ*, **712**, 274
- Nordstrom, B., et al. 2004, *A&A*, **418**, 989
- Olofsson, J., Juhász, A., Henning, Th., et al. 2012, *A&A*, **542**, A90
- Olsen, E. H., & Perry, C. L. 1984, *A&AS*, **56**, 229
- Osten, R. A., & Wolk, S. J. 2015, *ApJ*, **809**, 79
- Pecaut, M. J., Mamajek, E. E., & Bubar, E. J. 2012, *ApJ*, **746**, 154
- Preibisch, T., Kim, Y.-C., Favata, F., et al. 2005, *ApJS*, **160**, 401
- Raassen, A. J. J., Mewe, R., Audard, M., et al. 2002, *A&A*, **389**, 228
- Raymond, J. C., & Smith, B. W. 1977, *ApJS*, **35**, 419
- Raymond, S. N., Schlichting, H. E., Hersant, F., & Selsis, F. 2013, *Icar*, **226**, 671
- Rhee, J. H., Song, I., & Zuckerman, B. 2008, *ApJ*, **675**, 777
- Rosotti, G. P., Ercolano, B., & Owen, J. E. 2015, *MNRAS*, **454**, 2173
- Sartori, M. J., Lepine, J. R. D., & Dias, W. S. 2003, *A&A*, **404**, 913
- Shibata, K., & Yokoyama, T. 2002, *ApJ*, **577**, 422
- Smith, R., Wyatt, M. C., & Haniff, C. A. 2012, *MNRAS*, **422**, 2560
- Stauffer, J. R., Caillault, J.-P., Gagne, M., Prosser, C. F., & Hartmann, L. W. 1994, *ApJS*, **91**, 625
- Stern, R. A., Schmitt, J. H. M. M., & Kahabka, P. T. 1995, *ApJ*, **448**, 683
- Suchkov, A. A., Makarov, V. V., & Voges, W. 2003, *ApJ*, **595**, 1206
- Telleschi, A., Güdel, M., Briggs, K., et al. 2005, *ApJ*, **622**, 653
- Van Leeuwen, F. 2007, *A&A*, **474**, 653
- Voges, W., Aschenbach, B., Boller, Th., et al. 1999, *A&A*, **349**, 389
- Weinberger, A. J., Becklin, E. E., Zuckerman, B., & Song, I. 2004, *AJ*, **127**, 2246–51
- Wood, B. E., & Laming, M. J. 2013, *ApJ*, **768**, 122
- Wood, B. E., Müller, H.-R., Redfield, S., & Edelman, E. 2014, *ApJL*, **781**, L33
- Wood, B. E., Müller, H.-R., Zank, G. P., & Linsky, J. L. 2002, *ApJ*, **574**, 412
- Wood, B. E., Müller, H.-R., Zank, G. P., Linsky, J. L., & Redfield, S. 2005, *ApJL*, **628**, L143